ELSEVIER

Journal of Nuclear Materials 220–222 (1995) 330–335

journal of nuclear materials

UEDGE and DEGAS modeling of the DIII-D scrape-off layer plasma ☆

M.E. Fenstermacher [a], G.D. Porter [a], M.E. Rensink [a], T.D. Rognlien [a], S.L. Allen [a], D.N. Hill [a], C.J. Lasnier [a], T. Leonard [b], T. Petrie [b]

[a] *Lawrence Livermore National Laboratory, Livermore CA, USA*
[b] *General Atomics, San Diego CA, USA*

Abstract

This paper presents work to develop benchmarked theoretical models of scrape-off-layer (SOL) characteristics in diverted tokamaks by comparing shot simulations, using the UEDGE plasma fluid and DEGAS neutral transport codes, to measurements of the DIII-D SOL plasma. The experimental data include the radial profiles of n_e, T_e, and T_i, the divertor exhaust power, the intensity of H_α emission, and profiles of the radiated power. A very simple model of the anomalous perpendicular transport rates produces consistency between the calculated and measured radial profiles of the divertor power, and of the midplane densities and temperatures. Experimentally, the measured exhaust power is now 80–90% of the input power. The simulated peak power on the outer leg of the divertor floor is now within 20% of the measured power. Various sensitivities of these comparisons to model assumptions are described. Finally, these benchmarked models have been used to examine the effects of various baffle configurations for the radiative divertor upgrade in DIII-D.

1. Introduction

Predicting the performance of the divertor has been identified as a critical component of the design for future high power tokamaks like ITER and TPX. An active program is underway in both edge physics code development, and in validation of the code models against experimental data. Work on the former is described elsewhere [1]. This paper describes efforts to validate the complete 2-D solution from the UEDGE fluid code [2] against DIII-D experimental data. It also describes the application of UEDGE and the DEGAS neutral transport code [3] to design analysis for a radiative divertor program (RDP) upgrade of the DIII-D divertor.

☆ This work supported by the USDOE under contracts W-7405-ENG-48 at LLNL, and DEA-C093-89ERS51114 at General Atomics.

2. Validation of UEDGE with DIII-D data

This effort focusses beyond validation of the code solution for a single parameter or profile at a single location, in an attempt to simulate multiple diagnostic measurements at multiple locations in the SOL and divertor in a single code run. Simulation results are compared with the extensive SOL data set from DIII-D including measurements at multiple locations shown in Fig. 1 (eg. n_e and T_e from Thomson scattering and Langmuir probes, T_i from charge-exchange recombination (CER), P_{div} from IRTV, and the H_α emission from a photo diode array).

A very simple model of anomalous perpendicular diffusion for both particles and energy, with spatially constant diffusion coefficients, is used to compare the UEDGE SOL plasma simulation with the data. These diffusion coefficients, $D_\perp$, χ_i, and χ_e, are varied to fit the radial profiles of the measured upstream density and temperatures. Agreement is obtained with diffusion coefficients in the range $D_\perp \in (0.02, 0.25)$, and $\chi_{e(i)} \in (0.1, 0.5)$. The simulated midplane density and

Elsevier Science B.V.
SSDI 0022-3115(94)00494-3

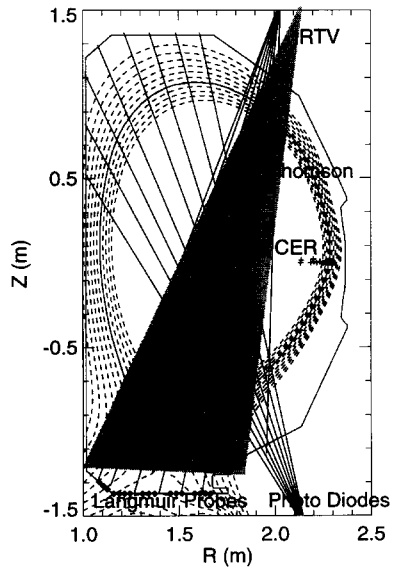

Fig. 1. SOL-relevant diagnostics on a typical single null discharge in DIII-D (1.0 cm flux surface spacing at the outer midplane).

temperature profiles are compared with data for an ELMing H-mode discharge in Fig. 2. Agreement exists within the uncertainty of the location of the separatrix (a few millimeters) except for the density in the very outer SOL.

The SOL plasma parameters are determined by the choice of the diffusion coefficients and by boundary conditions (eg. measured n_e and T_e at the innermost flux surface, plate recycling coefficients, and wall properties). The 2-D plasma solution is compared with data at several locations: first the calculated power across the separatrix is consistent with that measured (within 10% for the case of Figs. 2 and 3). Secondly, the calculated outer plate power profile agrees well with the experiment (Fig. 3a). The peak is somewhat higher, but the total power is actually 30% lower, than measured. The calculated power profile for the inner leg is substantially higher than measured. Finally, the calculated H_α emission for the outer divertor agrees well with the data (Fig. 3b). The H_α at the inner strike point is 50% higher than measured but it is lower than the data in the private flux region. Langmuir probe data near the strike points show higher T_e and lower n_e than calculated (by a factor of 3 at the outer and more than an order of magnitude at the inner strike point). Combining this with the H_α and power data suggests that the inner leg is detached experimentally while the code solution is still attached.

The discrepancies at the inner strike point may arise from radiation effects; impurities are only crudely included in these UEDGE simulations. A specified fraction of impurity atoms is assumed throughout the plasma, and the radiative electron energy loss in the plasma is self-consistently included. The non-equilibrium emissivity is calculated as a function of T_e using tabulated data from a series of MIST code runs [4]; charge exchange between impurity ions and neutral hydrogen is included in the MIST results, so the impurity charge state distribution and emissivity also depend on the neutral hydrogen density.

Including the radiative power loss from a small carbon concentration (0.6% for the case shown in Figs. 2 and 3) increases the in/out power asymmetry by more than a factor of 2. The power to the inner strike point is reduced by enhanced impurity radiation in the high n_e, low T_e plasma created by the long connection length from the outer midplane to the inner strike point. Over half of the remaining UEDGE power to the inner plate arises from recombination of the ion current in the plate. Experimentally, the plasma at the inner strike point is detached with low ion current to the plate (and hence very low power there). This effect

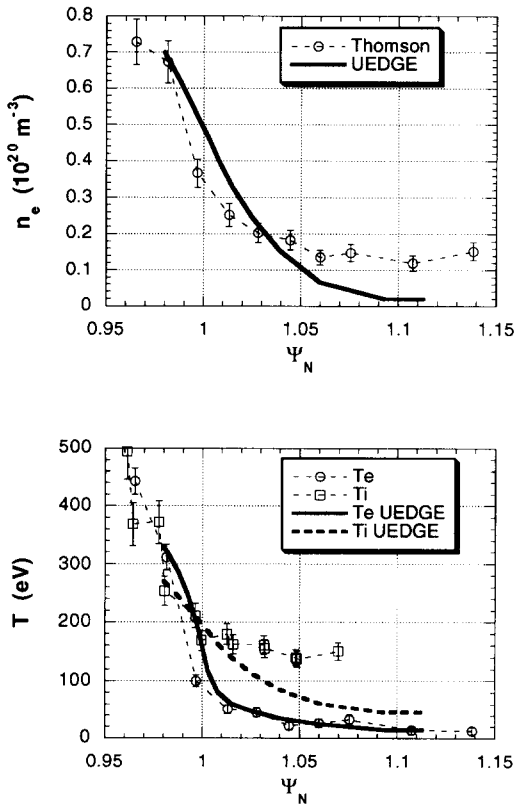

Fig. 2. Comparison of UEDGE results with data for the midplane density and temperature profiles in an ELM-free H-mode discharge.

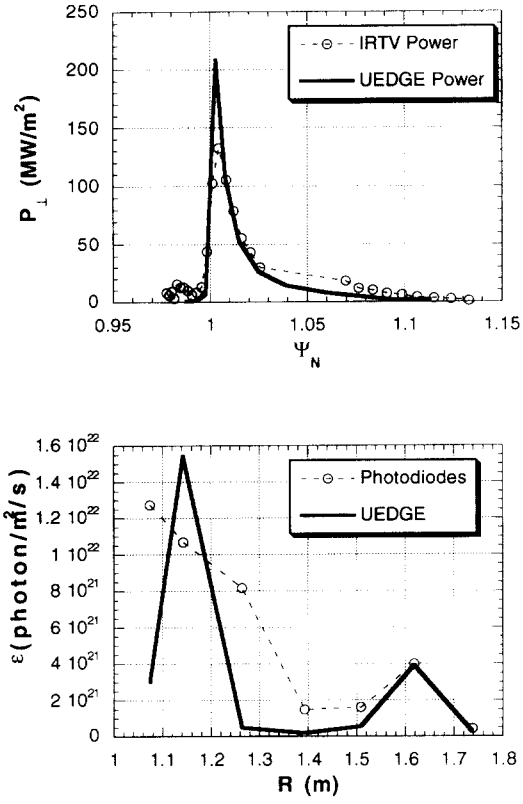

Fig. 3. Comparison of the UEDGE simulation results with data, (a) divertor power profile at the outer strike point and, (b) H_α emission profile across the divertor.

is not seen in present simulations, although it may be possible with an improved impurities model recently installed in UEDGE [2].

The quality of the UEDGE simulations in the areas of power balance, peak divertor power and radial profiles has improved significantly over previous work [2]. To improve the models in other areas, the sensitivities of the simulations to various assumptions have been explored. Results are summarized below.

- The in/out asymmetry of the divertor power is increased (inner power reduced) by including the effect of parallel currents in the SOL.
- The H_α emission in the private flux region is increased by increasing the plate recycling coefficient (R) from ~0.98 (used for the best simulations) to 1.0. However, the agreement between the measured and simulated emission near the strike points is poorer with $R = 1.0$.
- Variation in the UEDGE model of flux limits produces changes in the ion temperature near the divertor plate, a parameter not measured in the experiment.

3. Application to the radiative divertor

Present plans call for the installation of a new radiative divertor configuration in DIII-D in FY96 [5]. This should allow advanced divertor (i.e. reduced divertor heat flux) and advanced tokamak (AT) operation (i.e. controlled density in H- and VH-modes) simultaneously in DIII-D. The present ADP ring/baffle structure will be replaced with new structures which confine neutrals in the divertor region for the high triangularity AT shapes. UEDGE and DEGAS have been used to simulate the behavior of the plasma and neutral hydrogen in various generic shapes, and to guide engineering decisions to a conceptual design.

3.1. Plasma simulations with UEDGE for generic equilibria

The lower half of assumed up–down symmetric double null divertor configurations is modeled. Radial transport is anomalous with constant values for the particle and thermal diffusivities. The orthogonal mesh extends radially from a flux surface 0.3 cm inside the separatrix to a flux surface 3.5 cm outside the separatrix at the outboard midplane. Fixed plasma density (3.5×10^{19} m^{-3}) and temperature (175–200 eV) are specified on the innermost flux surface to obtain a total power flow of 9 MW across the separatrix. Zero-gradient boundary conditions are imposed at the outermost SOL flux surface and at the innermost private-flux surface. At the divertor plates, standard sheath boundary conditions and unity recycling for the ion particle flux striking the plate are applied. Pumping boundary conditions for the hydrogen neutrals at the private flux wall and outermost side walls of the mesh are specified by a fixed albedo of 0.95.

Three divertor configurations, with different plasma shapes characterized by the length of the outboard divertor leg (X-point to separatrix strike point) are compared: 40 cm, 20 cm and a "reference case". The particle and heat flux profiles at the outboard divertor plate are shown in Fig. 4. The peak plate electron temperatures were 16, 36 and 48 eV for the three cases, respectively. The longer slot length yields lower divertor plate temperatures, but higher peak heat fluxes because of the smaller radial expansion of the flux tube (from midplane to divertor plate).

With sufficient hydrogen gas puffing from the private flux side wall of the outboard divertor leg, a plasma "detachment" is observed from the outboard plate in the sense that the peak of the recycling ionization region moves upstream toward the X-point with increasing gas puff current. Fig. 4 also shows steady state results for the 20 cm configuration with moderate (1000 A, attached) and strong (2200 A, detached) gas puffing. Total (plasma + neutral) parallel pressure is

approximately constant along the separatrix, so as the plate temperature collapses with increasing gas, the plasma and/or neutral density rises. The total hydrogen radiation remains small (less than 20%) compared to the total power crossing the separatrix even for strong gas puffing. The radiative energy loss per ionization event is reduced to less than 5 eV for high density (1.0×10^{21} m^{-3}) low temperature (5 eV) plasmas due to efficient multi-step ionization processes. Thus, it appears that radiation from impurities is necessary to significantly reduce the total power flow to the divertor plates.

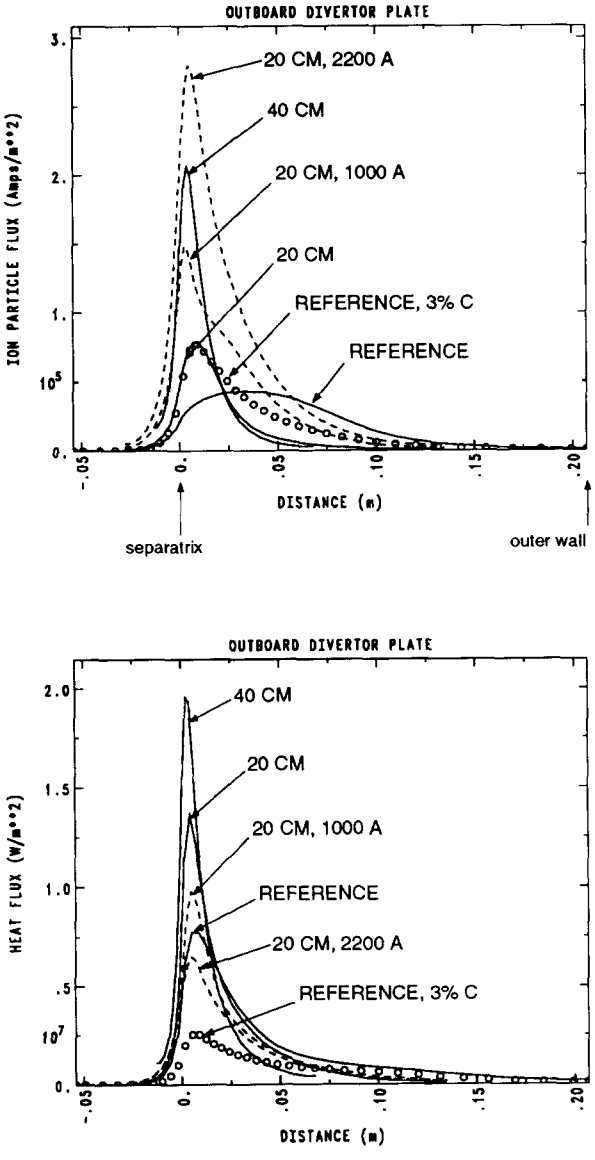

Fig. 4. Profiles on the outer plate calculated by UEDGE for the 20 cm, 40 cm and reference cases versus distance from the separatrix (mapped to the midplane): (a) particle flux and (b) heat flux.

3.2. Neutral transport with DEGAS for the generic equilibria

The figure-of-merit calculated by DEGAS for comparisons of candidate radiative divertor designs is the total ionization source (neutral current) inside the separatrix. Two processes contribute to this current: either neutrals leak radially out of the SOL in the divertor and penetrate the thin SOL plasma at the midplane, or a small fraction of the recycling current manages to propagate to the core against the divertor plasma flow. Scoping studies compared this core ionization source, I_{core}, to the neutral beam source in DIII-D (I_{nb} = 300–400 particle A at high power).

The scoping studies focussed on three questions: (1) how long must the baffled region be, (2) must the baffles be conformal to flux surfaces or would structures which slanted into the divertor plasma be sufficient, and (3) how narrow must the opening be near the divertor strikepoints? Baffle configurations used in the studies (Fig. 5) included close conformal walls, narrower conformal walls for which the recycling source at the top of the slot was taken into account, a "gas bag" configuration, and a completely open divertor (vacuum vessel only).

Two properties of the UEDGE solutions are important for many of the effects seen in the DEGAS simulations. First, for the radial profiles given in Fig. 4, a much larger recycled neutral flux occurs on a baffle intercepting a 1 cm flux line (mapped to the midplane) compared with the 2 cm flux line. Second, the ionization mean free path tends to be nearly a flux function except near the strikepoint, so neutrals in the outer SOL with velocities directed towards the separatrix have a much higher probability of ionization after a short flight than those directed along flux lines.

DEGAS simulations with all four generic baffles, using the UEDGE cases for the generic 20 cm and 40 cm X-point to outer strike point lengths, were compared (Table 1). As expected, the close conformal slot, without any recycling off the side walls or the top of the slot, produced the greatest reduction in I_{core}. A simple "gas bag" shape was sufficient in the 40 cm configuration to reduce the source well below the beam source, and was marginal in the 20 cm configuration. In the narrower slot the recycling off the top of the slot was an important source of core influx. This study showed that proper shaping of a baffle in a 20–30 cm configuration would be sufficient to reduce the core source below the beam source.

Conformal slots have many disadvantages including limited diagnostic access and reduced operational flexibility. Also the recycling from the top of the slot can

Table 1
Comparison of the core ionization currents (A) found for generic baffle designs with two plasma configurations

Configuration	20 cm	40 cm
Open	880 ± 57	711 ± 65
Gas bag	287 ± 33	73 ± 21
Close conformal	37 ± 12	5 ± 5
Narrower conformal with recycling	57 ± 15	92 ± 23

Table 2
Comparison of core ionization currents (A) for cases with and without deuterium gass puff (20 cm configuration, slanted baffle)

UEDGE plasma case	3.5 to 2.0 cm	2.0 to 1.0 cm	
		Unoptimized	Partially optimized
No gas puff	63 ± 15	160 ± 24	114 ± 21
1.0 kA D_2 puff	77 ± 24	263 ± 45	207 ± 40
2.2 kA D_2 puff	115 ± 37	264 ± 57	234 ± 54

produce a significant core source. For these reasons a slanted baffle geometry (Fig. 5) was examined. The surface intercepting plasma flow is slanted so that the emitted neutrals are directed toward the hotter regions of the SOL to be ionized and entrained by the plasma flow. Baffles with slanted surfaces crossing flux surfaces from 3.5 cm (outer boundary of the UEDGE plasma solution) to 2.0 cm off the separatrix were compared with tighter baffles spanning the 2.0 to 1.0 cm flux surfaces. The shape of the upper knee of the baffle was also varied. Each of these baffle configurations was simulated with DEGAS using three UEDGE plasma solutions in the 20 cm configuration; no puff, 1.0 kA puff (attached) and 2.2 kA puff (detached) (Table 2). Puffing does increase I_{core} somewhat. In the wider opening case, the core source at the maximum puff is still well below the beam source. With the narrower configuration the source rate approaches the beam rate in the highest puffing case, especially when the upper baffle region is not optimized, because the surfaces intercept regions of higher plasma flow (closer to the separatrix) at locations closer to the X-point. Finally, a noticeable decrease in the core source was observed with only a minor change in the shape of the upper knee of the baffle. Two conclusions can be made: (1) slanted baffles are a viable option since all of these configurations at least marginally satisfy the goal of reducing I_{core} below the beam source, and (2) a slanted baffle extending in to the 2.0 cm flux line is sufficiently narrow to control the neutral source; tighter

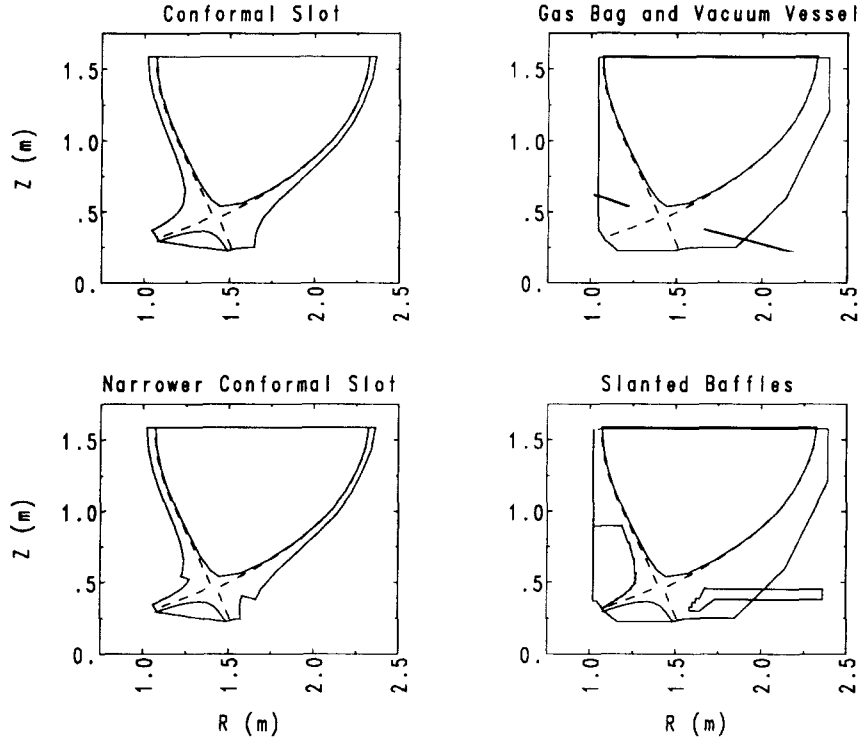

Fig. 5. Generic baffle configurations used in DEGAS for the RDP studies (separatrix shown as a dashed line); (a) conformal slot (b) "gas bag" baffles and the outer vacuum vessel, (c) a narrower conformal slot, and (d) slanted baffles.

baffles produce greater core source due to recycling from the upper part of the structure.

3.3. Analysis of the reference RDP configuration

The studies described above helped guide the development of a reference engineering design for the RDP. The reference design has an X-point to outer strikepoint length of 23 cm, a slanted outer baffle with a 1.0 cm opening near the strikepoint (chosen to optimize pumping performance), careful shaping of the upper knee of the baffle, a baffle on the 0.25 cm flux line in the private flux region and a cryopump for the private flux and inner strikepoint regions (see Ref. [5]).

The UEDGE result for this configuration is shown in Fig. 4. The corresponding DEGAS simulation produced a core ionization source of 65 ± 15 A, well below the beam source. In addition, a case showing the beneficial effect of impurity radiation, with carbon impurities artificially constrained to the regions near the divertor plates, is included in Fig. 4. The total power and peak power are significantly reduced (factor of 3) by a 3% carbon concentration. For this case the electron temperature is low enough that Z_{eff} of the plasma remains below 1.5 in the divertor region.

4. Conclusions and plans for continued work

A simple model of anomalous perpendicular diffusion of particles and energy (constant diffusion coefficients) produces good agreement between experimental measurements and UEDGE calculated plasma and heat flux profiles. Agreement within a factor of 2 is also achieved between the measured and calculated divertor H_α emission. Using this model in conjunction with DEGAS showed that the goals of the RDP upgrade for DIII-D could be met with a modest X-point to outer target length (20–30 cm) and a slanted baffle structure.

Near term plans include installation of algorithms for impurity transport and non-orthogonal grids in UEDGE [2], validation of DEGAS solutions against DIII-D H_α and neutral pressure data, benchmarking of UEDGE neutrals solutions against DEGAS, and continued analysis of optimal configurations for the RDP.

References

[1] D. Reiter, J. Nucl. Mater. 196–198 (1992) 80, and references therein.
[2] T.D. Rognlien et al., J. Nucl. Mater. 196–198 (1992) 347; G.R. Smith et al., Proc. 11th Int. Conf. on Plasma–Surface Interactions in Contr. Fusion Devices, Mito, Japan, 1994 (Elsevier, Amsterdam, 1994), to be published in J. Nucl. Mater.
[3] D.B. Heifetz et al., J. Comput. Phys. 46 (1982) 309.
[4] R. Hulse et al., J. Phys. B 13 (1980) 3895; R. Hulse, Nucl. Techn./Fusion 3 (1983) 259.
[5] S.L. Allen et al., Proc. 11th Int. Conf. on Plasma–Surface Interactions in Contr. Fusion Devices, Mito, Japan, 1994 (Elsevier, Amsterdam, 1994), to be published in J. Nucl. Mater.